Nuclear Instruments and Methods in Physics Research B 268 (2010) 476–480

Contents lists available at ScienceDirect

Nuclear Instruments and Methods in Physics Research B

journal homepage: www.elsevier.com/locate/nimb

Impedance studies on high energy Li^{3+} irradiated PZT thin films

Basavaraj Angadi [a], V.M. Jali [b,*], Ravi Kumar [c], S.B. Krupanidhi [d]

[a] Department of Physics, Bangalore University, Bangalore 560 056, India
[b] Department of Physics, Gulbarga University, Gulbarga 585 106, India
[c] Inter University Accelerator Centre, Aruna Asaf Ali Marg, New Delhi 110 067, India
[d] Materials Research Centre, Indian Institute of Science, Bangalore 560 012, India

ARTICLE INFO

Article history:
Received 18 June 2009
Received in revised form 20 November 2009
Available online 3 December 2009

Keywords:
Ferroelectric thin films
PZT
Ion irradiation
Impedance spectroscopy

ABSTRACT

The ferroelectric $Pb(Zr_{0.48}Ti_{0.52})O_3$ (PZT) thin films prepared by the pulsed laser deposition technique were studied for their response to high energy lithium ion irradiation through impedance spectroscopy. The Debye peaks, observed in the impedance and modulus plots of irradiated films, shifts towards higher frequencies compared to those of unirradiated films. This is equivalent to the trend observed with increase in temperature in the unirradiated films due to the dielectric relaxation. The irradiated films showed a decrease in the grain resistance compared to the unirradiated films. The activation energy of dielectric relaxation increases from 1.25 eV of unirradiated film to 1.62 eV of irradiated film. The observed modifications in the irradiated film were ascribed to the modifications in the grain structure due to the high value of electronic energy loss.

Introduction

Ferroelectric thin films are being studied extensively for their potential applications in the memory technology [1]. There has been continuous search for a suitable composition with high dielectric constant, high remnant polarization, low coercive field and with a better fatigue endurance for the present requirement in the commercial memory market. Lead Zirconate Titanate (PZT) has been studied for this purpose since long time [1,2]. Memory devices in the form of high density DRAMs and NVRAMs with PZT as a memory element are being fabricated and used extensively. In spite of earlier reports of radiation hardness [3,4], PZT has shown degradation in their properties after irradiation [5,6].

The radiation induced degradation in the properties of ferroelectric thin films has been explained in terms of the radiation theory: the pinning of ferroelectric domains by the radiation induced defects [6]. However, most of the work has been done on the bulk ceramics and few ferroelectric thin films for the X-ray, γ-ray and neutron irradiation [7–9]. There are very few reports of the high energy heavy ion induced irradiation effects on the ferroelectric thin films [6,10].

The irradiation can modify the various regions of the ferroelectric thin film capacitors, namely ferroelectric bulk and interfaces like ferroelectric-electrode and grain boundaries. It has been very difficult to isolate the contributions of these in the property changes after irradiation. In this regard, the impedance spectroscopy has been a powerful and well-known technique for investigating dielectric materials [11,12]. The contributions of various processes such as the electrode effects, bulk effects, and their interfaces (viz. the grain boundaries etc.) can be resolved in the frequency domain.

High-energy swift heavy ions, such as the Li^{3+} in the present case, lose their energy to the medium that leads to creation of defects and structural changes and there by alters their properties. A high energy heavy ion looses its energy in a medium through two processes, namely, electronic loss (S_e) and nuclear collisions (S_n). The latter process is the dominant mode of energy loss at low ion energies and peaks around 1 keV/u and is responsible for displacing atoms of the medium from their lattice positions. The electronic energy loss is appreciable at higher energy and peaks around 1 MeV/u. In this process the target atom is not displaced but only excited or ionized. However, it can also lead to displacement of lattice atoms in a cylindrical core along the ion path in insulating materials either through the coulombic explosion [13] or the thermal spike [14]. Along these latent tracks the material suffers amorphization because of which its properties are affected.

In this paper we are using the impedance spectroscopy to investigate the effect of 50 MeV Li ions on the properties of ferroelectric PZT thin films. The ferroelectric and the ac conductivity studies carried out on the same samples are published elsewhere [6,15].

2. Experimental

The PZT thin films were prepared by the pulsed laser deposition technique. Single phase bulk targets of $Pb(Zr_{0.48}Ti_{0.52})O_3$ prepared

* Corresponding author. Tel.: +91 9845633050; fax: +91 8472 263206.
E-mail address: vmjali@rediffmail.com (V.M. Jali).

0168-583X/$ - see front matter © 2009 Elsevier B.V. All rights reserved.
doi:10.1016/j.nimb.2009.11.011

by the conventional ceramic method were used. About 0.7 μm thick PZT films were deposited on platinum coated silicon substrates. The phase and the crystallinity were confirmed by using a Scintag X-ray diffractometer. Several gold electrodes of 2.6 × 10^{-3} cm^2 area were deposited on the top surface of the film using thermal evaporation technique and a physical mask. The complex impedance of the samples was measured using a computer interfaced Keithley 3330 meter in the frequency range 100 Hz–100 kHz and in the temperature range from 27 to 400 °C.

Li^{3+} ion irradiation (50 MeV) was carried out at room temperature using a 15 UD Pelletron Accelerator at Inter University Accelerator Centre (IUAC), New Delhi, India. The irradiation fluence, calculated by integrating the charges collected by the sample through the current integrator, was 1×10^{14} ions/cm^2. The incident ion beam was scanned over the entire area of the film by using a magnetic scanner to ensure the uniform irradiation across the film area. The impedance measurements were done again after the irradiation.

3. Results and Discussion

3.1. Impedance studies theory

Impedance spectroscopy has been widely used to characterize the dielectric materials. In this technique one or more of four possible formalisms, the impedance Z^*, the electric modulus M^*, the admittance Y^* and the permittivity ϵ^* have been used for the analysis. All these are interrelated [16]:

$$M^* = j\omega C_0 Z^*, \tag{1}$$

$$\varepsilon^* = (M^*)^{-1}, \tag{2}$$

$$Y^* = (Z^*)^{-1}, \tag{3}$$

$$Y^* = j\omega C_0 \epsilon^*, \tag{4}$$

where ω is the angular frequency (=$2\pi f$, with f the applied frequency in Hz), C_0 is the vacuum capacitance of the measuring cell and the electrodes with an air gap in place of the sample, $C_0 = \varepsilon_0 / k$, where ε_0 is the permittivity of free space (8.854×10^{-14} F/cm), and $k = l/A$, the cell constant where l is the thickness and A the area.

The analysis and the interpretation of the experimental data will be easier with an equivalent circuit model that represents the electrical system under study. This is chosen based on (i) intuition as to what kind of impedances are expected to be present in the sample and whether they are connected in series or parallel, (ii) examination of the experimental data to see whether the response is consistent with the proposed circuit, and (iii) inspection of the resistance and capacitance values that are realistic and that their temperature dependence, if any, is reasonable [12].

A material consisting of the regions of bulk, grain boundary and material/electrode interfaces can be represented by three parallel RC elements connected in series [17]. Each parallel RC element results in a semicircle in the impedance, Z^*, and the electric modulus, M^*, complex plane plots and in a Debye peak in spectroscopic plots of the imaginary components, Z'' and M'' vs. log f. The Debye peak in Z'' and M'' spectra is described by

$$Z'' = \mathrm{R}\left[\frac{\omega \mathrm{RC}}{1 + (\omega \mathrm{RC})^2}\right], \tag{5}$$

$$M'' = \frac{\varepsilon_0}{C}\left[\frac{\omega \mathrm{RC}}{1 + (\omega \mathrm{RC})^2}\right]. \tag{6}$$

The frequency at the semicircle maxima, ω_{max}, and correspondingly, at the Debye peak maxima, for each RC element is given by

$$\omega_{max} = 2\pi f_{max} = (\mathrm{RC})^{-1} = \tau^{-1} \tag{7}$$

where the product RC is the time constant, ,τ of the RC element; τ and, therefore f_{max} are intrinsic properties of the RC element, because they are independent of geometry. The magnitudes of the Debye peaks scale accordingly to R for Z'' spectra (Eq. (5)) and C^{-1} for M'' spectra (Eq. (6)). Consequently, Z'' spectra (and Z^* plots) are dominated by those RC elements with the largest R values, where as M'' spectra (and M^* plots) are dominated by those with the smallest C values. The low capacitance regions, such as grain interiors, are characterized using M'' data, whereas more resistive regions, such as grain boundaries and electrode interfaces, which often have higher associated capacitances, are characterized using Z'' spectra. An advantage of a combined M'', Z'' plot is that the M'', Z'' peaks for a particular RC element should be coincident on the frequency scale. When no M'' peak maxima could be obtained, the associated resistance could some times be estimated from the non-zero, high frequency intercept on the Z'' axis of the Z^* plots.

3.2. Unirradiated studies

The impedance spectroscopic plots of Z'' vs. frequency and M'' vs. frequency for unirradiated PZT thin films in the temperature range from 300 to 360 °C are shown in Fig. 1. The plots show the characteristic Debye peaks at different frequencies and the peak position is found to shift towards the high frequency side with increasing temperature. Below 300 °C, the films showed no observable Debye peaks in the measured frequency range. This could be due to the higher relaxation times associated with the dielectric relaxation mechanism at lower temperatures up to 300 °C. As the film temperature was increased above 300 °C, the Debye peak starts appearing in the measured frequency range. The shift of peak position towards the higher frequency side with temperature imply that the relaxation time decreases at higher temperatures. It is also clear from the figure that irrespective of the measured temperatures, all the curves at high frequencies were merging with

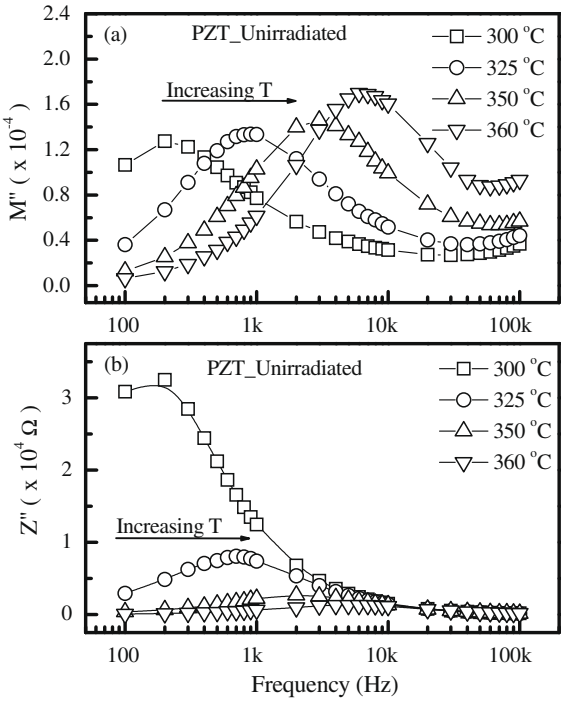

Fig. 1. Variation of (a) imaginary part of the modulus, M'' with frequency, (b) imaginary part of the impedance, Z'' with frequency, for the unirradiated PZT thin film.

one another. Materials with charge carriers are known to exhibit such type of temperature and the frequency dependence. At higher frequencies, the bulk grain dispersion predominated due to the diminishing of the space charge effects as their relaxation times were very high compared to the bulk grains. The combined plot of Z'' and M'' vs. frequency at 300 and 325 °C are shown in Fig. 2 for an unirradiated PZT thin film. The plots show that the impedance and the modulus peaks are broader and asymmetric and the peak positions are not exactly at the same frequency, which represents the deviation from the ideal Debye relaxation phenomena. According to the ideal Debye's theory of relaxation, the impedance (Z'') and the modulus (M'') should peak at the same frequency for a given and/or measured temperature. The half height peak width is observed to be nearly 1.1 decades, which for the ideal case should be 1.14 decades [16].

The complex impedance and modulus plane plots for the unirradiated PZT thin film are shown in Figs. 3 and 4 respectively. The single semicircle observed in the complex impedance plots at lower temperatures reveals that the response is from the single RC combination corresponding to bulk grain behavior. However, when the temperature was increased, the grain boundary effect started appearing in the form of unresolved second semicircle, as shown in the inset of Fig 4, which can be seen at lower frequencies. The appearance of the second unresolved peak indicates the superposition of various distributed relaxation times. This high temperature behavior can be described by the series combination of two parallel RC circuit elements corresponding to the dielectric behavior of the interior grain and the grain boundary. Since the grain boundaries exhibit normally high resistance than the grain interiors, the first semicircle in the high frequency region could be attributed to the behavior of grain interior while the second unresolved semicircle in the low frequency region is attributed to the grain boundaries. The complex modulus plots also showed the contribution of the both grain and the grain boundaries.

3.3. Lithium irradiation effects

The impedance spectroscopic plots of Z'' vs. frequency and M'' vs. frequency for lithium irradiated PZT thin films in the tempera-

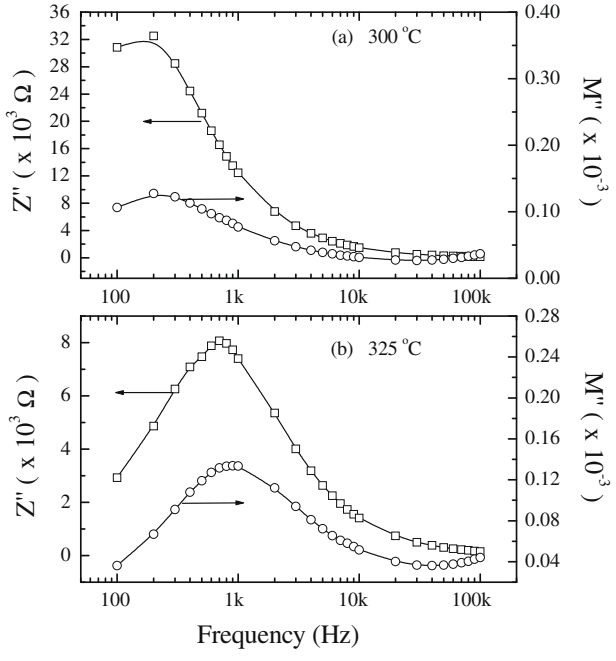

Fig. 2. The combined plot of Z'' and M'' vs. frequency at (a) 300 °C and (b) at 325 °C, for the unirradiated PZT thin film.

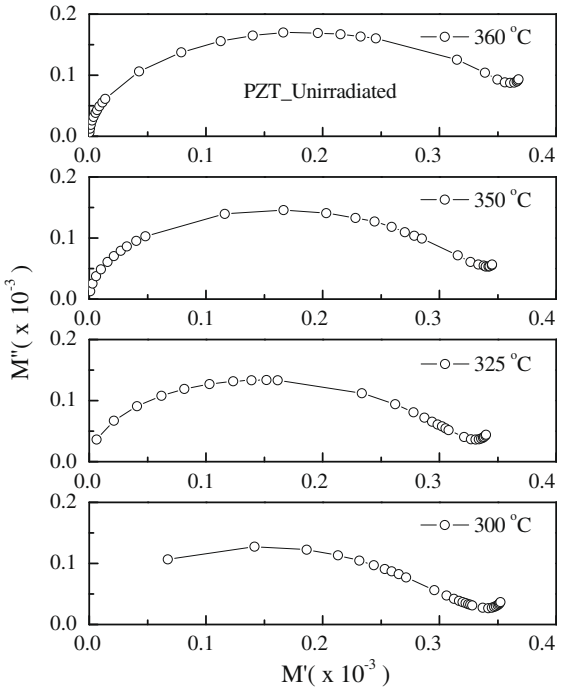

Fig. 3. The complex modulus plane plots for the unirradiated PZT thin film.

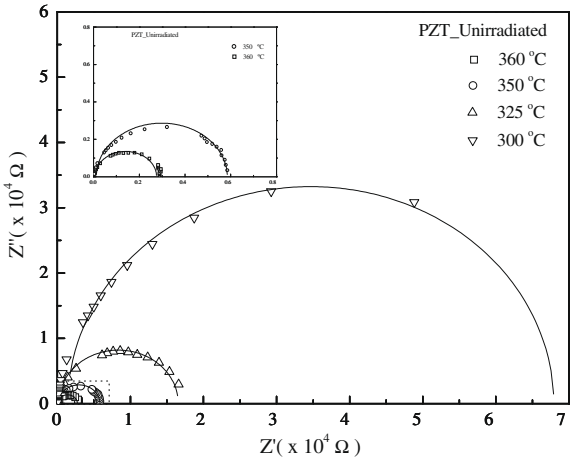

Fig. 4. The complex impedance plane plots for the unirradiated PZT thin film. The inset shows enlarged plots of the same film at temperatures 350 and 360 °C.

ture range from 200 to 300 °C are shown in Fig. 5. The characteristic Debye peaks started appearing from 250 °C itself and the peak position was found to shift towards the high frequency side with increasing temperature. At 300 °C, the Debye peak appeared at 20 kHz which had appeared at 200 Hz for the unirradiated film. That means, at a given or measured temperature, the Debye peaks are observed to be shifted towards higher frequencies after irradiation. This shows that there is a decrease in the relaxation time after irradiation. This is equivalent to the effect observed due to increase in the temperature as discussed in Section 3.2.

The combined plot of Z'' and M'' vs. frequency at 275 and 300 °C are shown in Fig. 6 for lithium irradiated PZT thin film, which also showed the deviation from the ideal Debye behavior. The modulus plot of the irradiated film shows the appearance of two peaks at lower temperatures (275 °C). This shows that the response corresponds to the two parallel RC combinations, one of bulk grain and the other of grain boundaries. The grain boundary response

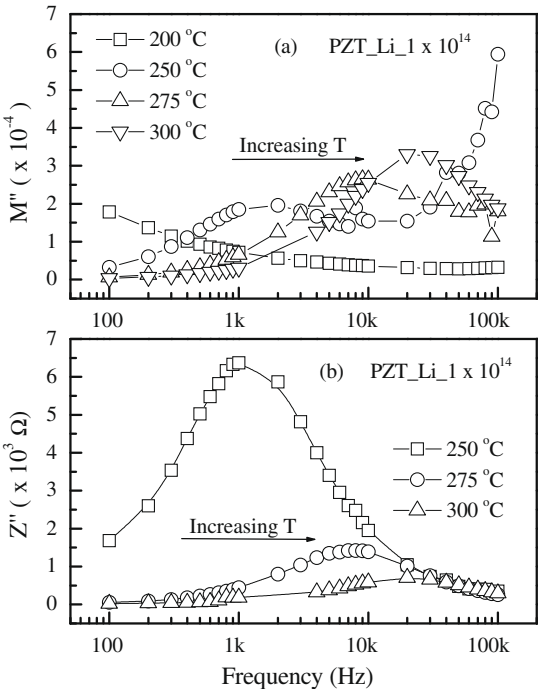

Fig. 5. Variation of (a) imaginary part of the modulus, M'' with frequency, (b) imaginary part of the impedance, Z'' with frequency, for the Li irradiated PZT thin film.

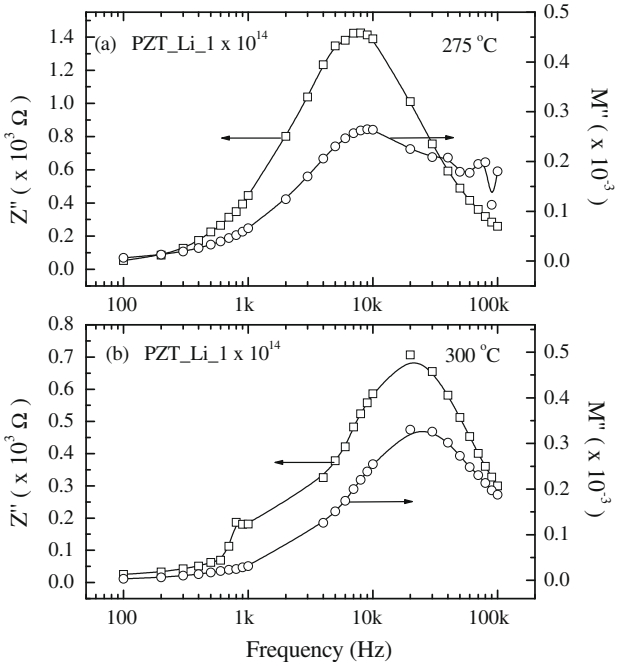

Fig. 6. The combined plot of Z'' and M'' vs. frequency at 275 and 300 °C for Li irradiated PZT thin film.

at lower temperatures in the irradiated films is due to radiation induced degradation at the grain boundaries along with the grain interior.

The complex impedance and modulus plane plots for the lithium irradiated PZT thin film are shown in Figs. 7 and 8 respectively. The grain resistance, intercept on the Z'' axis of the semicircle, observed to be decreased when compared to the unirradiated film. This may be due to the radiation induced conducting paths both

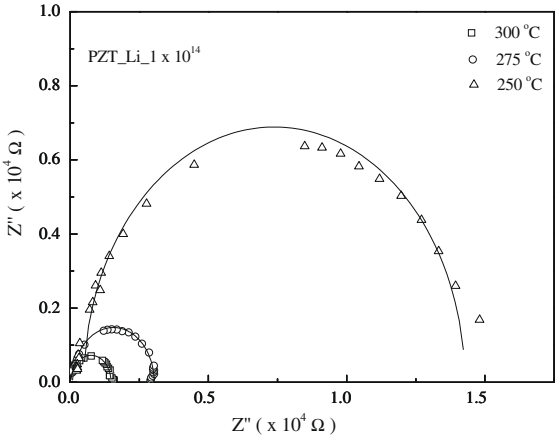

Fig. 7. The complex impedance plane plots for the Li irradiated PZT thin film.

within the grain and at the grain boundaries. The modulus plots of irradiated films showed the grain boundary effects at lower temperatures (viz. 250 and 275 °C) than the unirradiated film. This again proves that the radiation induced modification occurs both at the grain boundaries and the grain interiors.The activation energy for dielectric relaxation was calculated using the following expression:

$$\omega_p = \omega \exp(-E_t/kT)$$

where E_t is the activation energy for dielectric relaxation, T being the absolute temperature and ω_p is the peak angular frequency. The Arhenius plots of ln ω_p vs. (1000/T) for both the unirradiated and the irradiated films are shown in Fig. 9. The activation energies for dielectric relaxation were calculated from these Arhenius plots for both the unirradiated and the irradiated films. The unirradiated films showed activation energy of 1.25 eV and is increased to 1.62 eV after irradiation. These values are in agreement with our earlier results obtained using ac conductivity measurements [15]. The high value of electronic energy loss (S_e), about two orders of magnitude higher compared to the nuclear energy loss (S_n), is

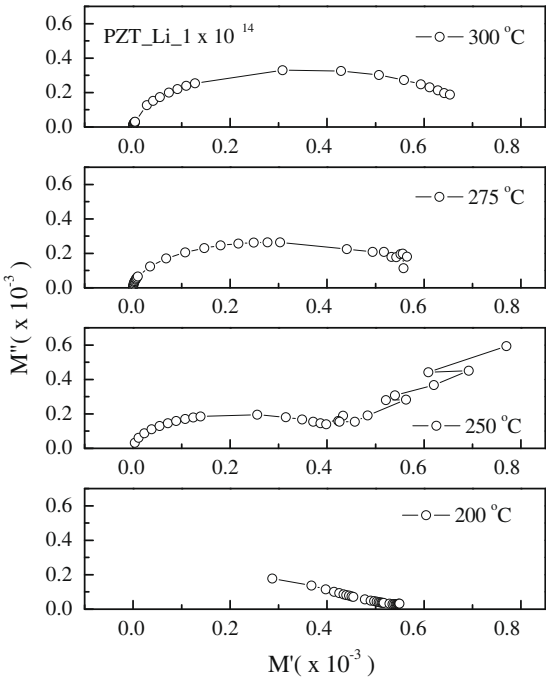

Fig. 8. The complex modulus plane plots for the Li irradiated PZT thin film.

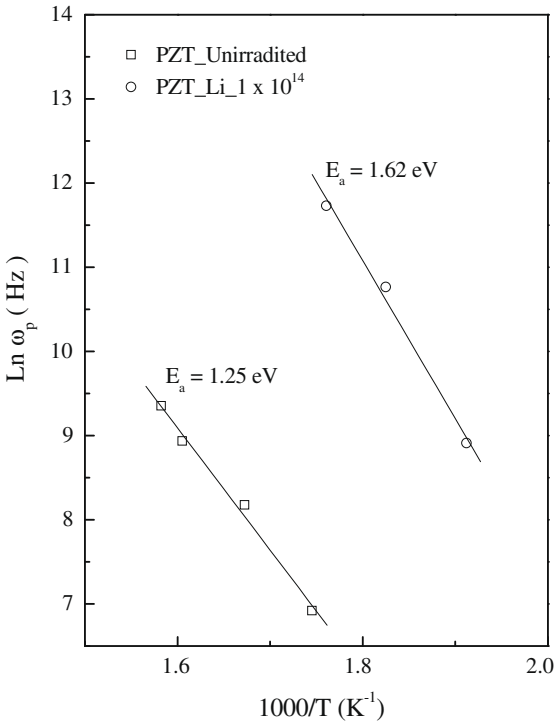

Fig. 9. The Arhenius plots of ln ω_p vs. (1000/T) for both the unirradiated and the Li irradiated PZT thin film.

mainly responsible for the observed changes in the properties of irradiated films [6].

4. Conclusions

In conclusion, the ferroelectric PZT thin films were prepared by the pulsed laser deposition technique and the effect of 50 MeV lithium ion irradiation on these films were studied through impedance spectroscopy. The characteristic Debye peaks in the impedance and modulus plots are observed to be shifted towards higher frequencies after irradiation, implying the decrease in the relaxation time. The changes in the impedance and modulus plots of irradiated films reveal that the increased contribution from both the grain interior and the grain boundaries after irradiation is due to the radiation induced modifications both within the grain and at grain boundaries. Observed increase in the activation energy is in agreement with our earlier reported results obtained using ac conductivity measurements.

References

[1] J.F. Scott, C.A. Paz de Araujo, Science 246 (1989) 1400.
[2] T. Sakuma, S. Yamamichi, S. Matsubara, H. Ymaguchi, Y. Miyasaka, Appl. Phys. Lett. 57 (1990) 2431.
[3] T.F. Wrobel, J.A. Bullington, L.J. Schwee, GOMAC Digest of papers 13 (1987) 267.
[4] G.C. Messenger, F.N. Coppage, IEEE Trans. Nucl. Sci. NS-35 (1988) 1461.
[5] J.F. Scott, C.A. Araujo, H. Bret Meadows, L.D. McMillan, A. Shawabkeh, J. Appl. Phys. 66 (1989) 1444.
[6] Basavaraj Angadi, P. Victor, V.M. Jali, M.T. Lagare, Ravi Kumar, S.B. Krupanidhi, Thin Solid Films 434 (2003) 40.
[7] Y.M. Coic, O. Musseau, J.L. Leray, IEEE Trans. Nucl. Sci. 41 (3 Pt.1) (1994) 495.
[8] S.C. Lee, G. Teowee, R.D. Schrimpf, D.P. Birnie, D.R. Uhlmann III, K.F. Galloway, IEEE Trans. Nucl. Sci.39 (6 Pt.1) (1992) 2036.
[9] V.M. Jali, S. Aparna, Ganesh Sanjeev, S.B. Krupanidhi, Nucl. Instr. and Meth. in Phys. Res. B 257 (2007) 505.
[10] V.M. Jali, Basavaraj Angadi, P. Venkateshwarlu, Ravi Kumar, S.B. Krupanidhi, Nucl. Instr. and Meth. in Phys. Res. B 260 (2007) 553.
[11] D.C. Sinclair, A.R. West, J. Mater. Sci. 29 (1994) 6061.6.
[12] D.C. Sinclair, A.R. West, J. Appl. Phys. 66 (1989) 3850.
[13] D. Lesueur, A. Dunlop, Radiat. Eff. Def. Sol. 126 (1993) 163.
[14] G. Szenes, Phys. Rev. B. 51 (1995) 8026.
[15] Basavaraj Angadi, P. Victor, V.M. Jali, M.T. Lagare, Ravi Kumar, S.B. Krupanidhi, Mater. Sci. Eng. B 100 (2003) 93.
[16] I.M. Hodge, M.D. Ingram, A.R. West, J. Electroanal. Chem 74 (1976) 125.
[17] Finlay D. Morrison, Derec C. Sinclair, A.R. West, J. Am. Ceram. Soc. 84 (2001) 531.